Experimental Neurology 320 (2019) 113013

Contents lists available at ScienceDirect

Experimental Neurology

journal homepage: www.elsevier.com/locate/yexnr

Review Article

Anatomical imaging of the piriform cortex in epilepsy☆

James C. Young[a,b,*], David N. Vaughan[a,b,c], Helen M. Nasser[a,b,d], Graeme D. Jackson[a,b,c]

[a] The Florey Institute of Neuroscience and Mental Health, Melbourne Brain Centre, 245 Burgundy Street, Heidelberg, Victoria 3084, Australia
[b] Florey Department of Neuroscience and Mental Health, The University of Melbourne, Melbourne, 30 Royal Parade, Parkville, Victoria 3052, Australia
[c] Department of Neurology, Austin Health, Melbourne, 145 Studley Road, Heidelberg, Victoria 3084, Australia
[d] ISN Psychology - Institute for Social Neuroscience, Unit 15, 443 Upper Heidelberg Rd, Ivanhoe, Victoria 3084, Australia

ARTICLE INFO

Keywords:
Piriform cortex
Epilepsy
Imaging

ABSTRACT

The piriform cortex is a distinct brain region that plays a key role in the sense of smell. The piriform cortex is the major part of primary olfactory cortex and has broad connections that extend beyond the olfactory regions into limbic and fronto-temporal cortical networks. Numerous studies have described these anatomical connections via microscopic imaging and tracer studies. More recently, macroscopic anatomical imaging studies have demonstrated changes in the piriform cortex in humans with focal epilepsy as well as in animal models, suggesting this brain region can play a critical role in epileptogenesis. This review examines the imaging methods and techniques that have been most informative, leading to our current understanding of the anatomy and subdivsions of the piriform cortex as well as its connections to other brain structures, and the abnormalities that can be detected in the setting of epilepsy.

1. Introduction

The piriform cortex is a phylogenetically old brain region that plays a key role in our sense of smell. Piriform cortex is the largest component of primary olfactory cortex (Haberly, 1985; Haberly and Price, 1978; Löscher and Ebert, 1996). Confusingly the terms “prepiriform” and “prepyriform” have also been used to refer to the entire piriform cortex (Allison, 1954) or just the anterior piriform cortex (Klockgether et al., 1989). Primary olfactory cortex is defined by receiving direct input from the lateral olfactory tract. In addition to the piriform cortex this comprises the anterior olfactory nucleus, olfactory tubercle, periamygdaloid cortex and the anterior part of the entorhinal cortex (Carmichael et al., 1994). Extending beyond the piriform cortex, the broader olfactory network includes orbitofrontal cortex, thalamus and insular cortex (Shipley and Reyes, 1991) as well as interactions with other major cognitive networks. It has unique anatomical and functional properties that enable this role, but these very features may also predispose the piriform cortex to critical involvement in focal epilepsy. In this review we provide an overview of the anatomical location and subdivisions of the piriform cortex, its histological structure observed via staining, and its anatomical connections revealed through microscopic anatomical imaging. We also describe the various macroscopic imaging methods implemented in the study of the piriform cortex in epilepsy including magnetic resonance imaging (MRI) and nuclear medicine. Finally we discuss the key findings of these macroscopic anatomical imaging studies of humans with epilepsy and epilepsy animal models involving the piriform cortex.

2. Overview of piriform cortex and subdivisions

In humans, the piriform cortex is situated at the intersection of the frontal and temporal lobes, medial to the temporal stem (Mai, 2008), where it lines the superior and inferior banks of the entorhinal sulcus. It has a U-shaped cross section in coronal sections curving around the middle cerebral artery. It is a relatively small structure in humans, but relatively larger in mammals, where it was named for its pear-shaped appearance (Löscher and Ebert, 1996).

Piriform cortex can be divided into frontal (anterior) and temporal (posterior) parts (Fig. 1A and B), with each having distinct anatomical projections and specialized functional roles. In humans, the frontal lobe component of the piriform cortex lies lateral to the olfactory tubercle and the lateral olfactory tract, forming a triangular region posterior to orbitofrontal cortex and medial to insular neocortex (Allison, 1954; Porter et al., 2005). The temporal lobe component of the piriform cortex spreads from the limen insulae at the most anterior part of the temporal stem, and posteriorly to cover the amygdaloid nuclei

☆ This manuscript is part of a special issue “The Piriform Cortex in Epilepsy”.

* Corresponding author at: The Florey Institute of Neuroscience and Mental Health, Melbourne Brain Centre, 245 Burgundy Street, Heidelberg, Victoria 3084, Australia.
E-mail address: james.young@unimelb.edu.au (J.C. Young).

https://doi.org/10.1016/j.expneurol.2019.113013
Received 4 February 2019; Received in revised form 8 June 2019; Accepted 15 July 2019
Available online 16 July 2019

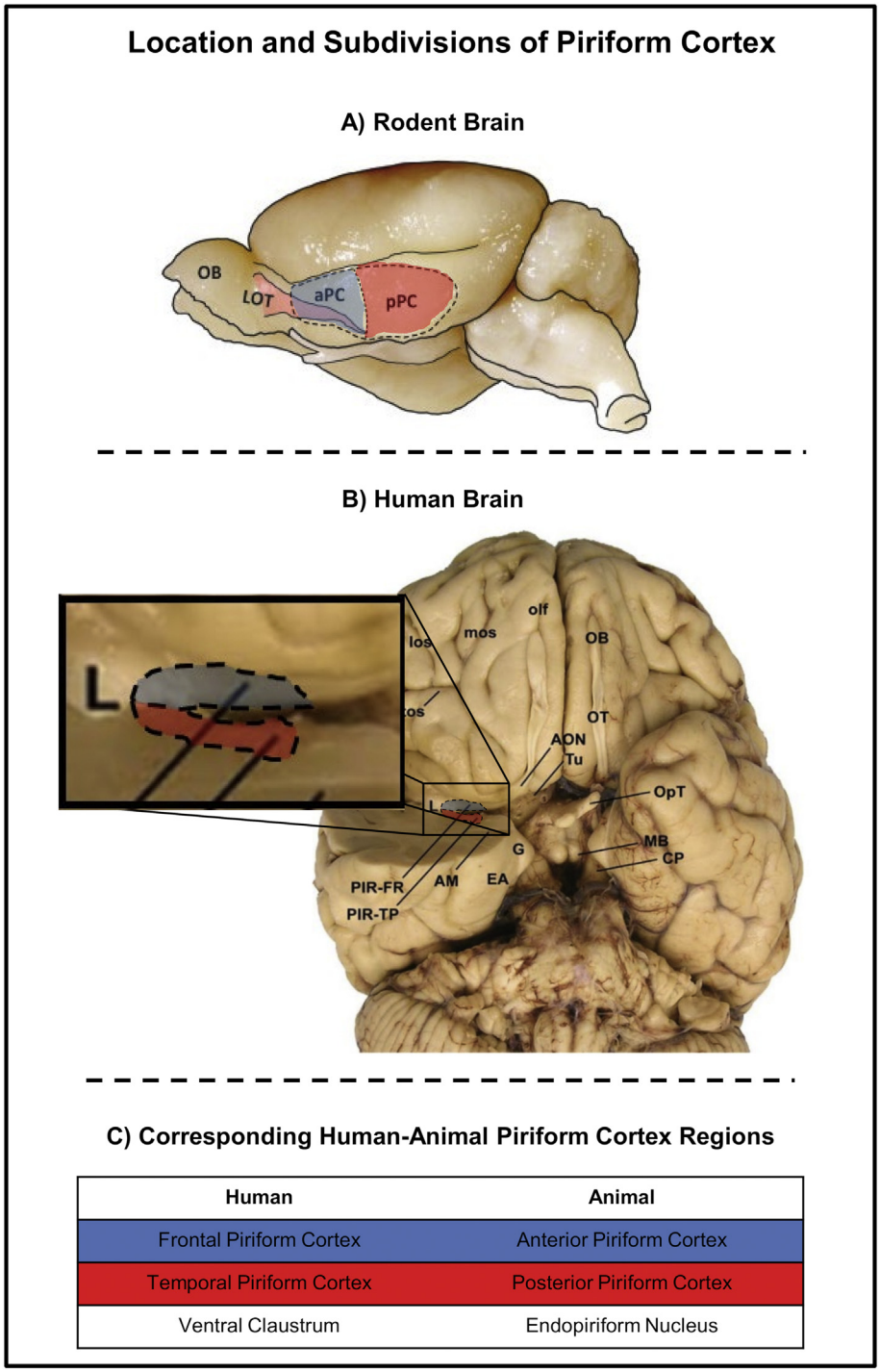

Fig. 1. Location of Piriform Cortex in Rat and Human Brains. A) Rat brain tilted to reveal ventral surface with approximate boundaries of anterior piriform cortex (aPC) and poster piriform cortex (pPC) as well as the olfactory Bulb (OB) and lateral olfactory tract (LOT). B) View of human ventral forebrain and medial temporal lobes. The right medial temporal lobe has been resected horizontally through the midportion of the amygdala (AM) to expose the frontal component of piriform cortex (PIR-FR) and temporal component of piriform cortex (PIR-TP). AON, anterior olfactory nucleus; CP, cerebral peduncle; EA, entorhinal area; G, gyrus ambiens; L, limen insula; los, lateral olfactory sulcus; OB, olfactory bulb; Opt, optic tract. A) was reproduced from (Bekkers and Suzuki, 2013) and B) was adapted from (Gottfried and Zald, 2005) with permission.

(Gonçalves Pereira et al., 2005) where it neighbours the cortical amygdala. The piriform cortex medially merges into perirhinal/entorhinal cortex and laterally into the insular neocortex (Mai, 2008). When viewing an MRI aligned to the conventional anterior commissure-posterior commissure axes, the piriform cortex is most easily visualized in the coronal plane, in the slices surrounding the slice that contains the anterior commissure (Fig. 6).

The rat piriform cortex lies on the inferolateral brain surface, ventral to the rhinal fissure. Its anterior component lies rostrally and its posterior component lies caudally, lateral to the amygdala (Paxinos and Watson, 1998). This anterior-posterior division is based on the thickness of cell layer III of the piriform cortex and on the presence (anterior) or absence (posterior) of the overlying lateral olfactory tract (Fig. 1A) (Löscher and Ebert, 1996). Here the lateral olfactory tract overlying the anterior piriform cortex is analogous to the relative position of these structures in the human frontal lobe. The posterior piriform cortex neighbours the amygdaloid nuclei (the basomedial amygdaloid nucleus followed more posteriorly by the basolateral amygdaloid nuclei), again similar to the relationship of temporal lobe piriform cortex to the amygdala in humans. In rats the agranular insular cortex is proximal to anterior piriform cortex before it caudally transitions into the entorhinal cortex where it lies proximal to the posterior piriform cortex (Paxinos and Watson, 1998). This is similar to the medial transition of the temporal lobe component of the piriform cortex into the perirhinal and entorhinal cortex and the lateral transition of the frontal lobe component into the insular neocortex. In imaging the piriform cortex in

a rodent, the sagittal plane is best for observing the transition between the anterior and posterior components as well as the three distinct layers. However, for observing the transition of the piriform cortex to neighbouring structures such as the amygdala and entorhinal cortex, the coronal plane is preferable.

The endopiriform nucleus is a subregion of the piriform cortex of particular importance. It lies deep to the piriform cortex along its entire rostrocaudal extent leading it to sometimes being referred to as layer IV of the piriform cortex. In rodents it spans the anterior and posterior extent of the piriform cortex and can accordingly be separated into dorsal and ventral parts (Behan and Haberly, 1999). The dorsal part of the endopiriform nucelus lies deep to the anterior piriform cortex whilst the ventral part lies deep to the posterior piriform cortex (Paxinos and Watson, 1998). The dorsal endopiriform nucleus displays parallel sensory and motor connections to the claustrum in rats (Behan and Haberly, 1999; Ekstrand et al., 2001; Watson et al., 2016) and exhibits less densely packed neurons compared to the ventral endopiriform nucleus. Together the dorsal and ventral parts of the rodent endopiriform nucleus are considered to serve similar functions as the ventral claustrum in humans (Brian, 2014; Kowiański et al., 1999). The endopiriform nucleus in rats and ventral claustrum in humans are both associated with processing sensory information via its interactions with prefrontal, cingulate, auditory, visual and somatosensory cortices, and is positioned deep to the frontal (anterior) component of the piriform cortex in humans (Dillingham et al., 2017; Mai, 2008; Paxinos and Watson, 1998; Sugai et al., 2012). The dorsal endopiriform nucleus in rats and ventral claustrum in humans both displays similar morphological characteristics, such as less densely packed neurons, as well as similar connections to the limbic system are similar (Kowiański et al., 1999).

There are two further subregions of the piriform cortex which have been defined in the animal kindling literature, namely the “central piriform cortex” and “area tempestas”. The central piriform cortex has been proposed as the transition zone between the anterior and posterior parts. Here the lateral olfactory tract disappears, there is an increase in cell layer III and the ventral endopiriform nucleus emerges (Löscher and Ebert, 1996; Schwabe et al., 2004). The area tempestas is a piriform cortex subregion defined on the basis of sensitivity to chemical stimulation and is not defined anatomically. It is located deep to the anterior piriform cortex, overlapping piriform layer III and the endopiriform nucleus (Gale, 1988). This region is highly sensitive to chemical stimulation of seizures, which can be induced by picomolar chemoconvulsant exposure. Induced seizures from area tempestas recruit epileptic activity within both anterior and posterior parts of the piriform cortex, highlighting the critical role of this deep region in seizure generation and propagation (Piredda and Gale, 1985).

3. Microscopic anatomical imaging of the piriform cortex

Microscopic imaging of the piriform has informed us about its cellular structure and neuronal connectivity. The piriform cortex has a distinct trilaminar structure (Fig. 2) (Haberly, 1985) consisting of highly interconnected pyramidal cells, inhibitory GABAergic interneurons and a horizontal arrangement of fiber projections.

Photomicrographs were originally used to visualize the various neurons of the piriform cortex (Haberly, 1985) however modern techniques typically utilize confocal or two-photon microscopy to classify neurons and detect morphological differences (Suzuki and Bekkers, 2006, 2010). Suzuki and Bekkers, 2006 used a combination of electrophysiology (in vitro), and calcium imaging (Suzuki and Bekkers, 2006). Layer I is the most superficial (at the surface of the endorhinal sulcus), has a relatively sparse cellular population, and receives input fibers from the lateral olfactory tract. Layer II contains densely packed somata of glutamate-releasing principal neurons whilst Layer III is the deepest layer also containing pyramidal neurons but at a lower density (Bekkers and Suzuki, 2013). Commissural and associational fibers are limited to Layer II and III (Neville and Haberly, 2004). Below Layer III lies the ventral claustrum or endopiriform nucleus which is directly connected to the piriform cortex (Hagiwara et al., 2012).

The three main excitatory neuron types within piriform cortex are the superficial pyramidal cells, deep pyramidal cells and semilunar cells. The pyramidal cells are tightly packed in layer IIb and more dispersed in layer III, with dendrites projecting up to layer I to receive inputs from the olfactory bulb (Neville and Haberly, 2003). Pyramidal cells are highly interconnected by recurrent projections onto many other pyramidal cells (Haberly, 1985). In rodents, a pyramidal cell has a dendritic arbour that extends over much of the piriform cortex and synapses with more than 1000 other cells (Barnes et al., 2008). Semilunar cells are a unique population located in layer 2a. They also receive olfactory bulb inputs, and are similar to pyramidal cells but do not have basal dendrites and show a distinct firing pattern (Neville and Haberly, 2003; Suzuki and Bekkers, 2006). Notably, layer II semilunar cells and superficial pyramidal cells have distinct projection patterns with the olfactory bulb and olfactory cortical regions which is mediated by a hierarchical feedback circuit (Mazo et al., 2017).

Inhibitory GABAergic cells are the predominant interneurons of the piriform cortex and they are found across all layers. Suzuki and Bekkers (2010) utilized molecular markers and confocal microscopy to classify the various classes of GABAergic interneurons of the piriform cortex, each demonstrating specific morphological and electrophysiological properties (Suzuki and Bekkers, 2010; Young and Sun, 2009). These interneurons provide both feed-forward and feedback inhibition onto the pyramidal cells in the piriform cortex (Franks et al., 2011; Luna and Schoppa, 2008; Stokes and Isaacson, 2010; Suzuki and Bekkers, 2012), which allows the pyramidal cells to produce temporally sparse but accurate responses to spike inputs received from the olfactory bulb. Suzuki and Bekkers (2010) used a glutamic acid decarboxylase (GAD) transgenic model and immunohistochemistry to identify different classes of GABAergic neurons in the different layers of anterior piriform (Suzuki and Bekkers, 2010). Specifically, they identified severely GABA cell types that may be specialized in fast, phasic inhibition and depending on input may mediate feedforward or feedback inhibition and other GABA cell types that may be involved in shaping inhibition along the somatodentric axis. These types of cells are differentially distributed amongst the layers within anterior piriform cortex. The equilibrium of excitation and inhibition in the piriform cortex is mediated by pre- and postsynaptic activation of $GABA_B$ receptor on GABAergic interneurons as they can both dampen and promote excitability (Gerrard et al., 2018). In the anterior piriform cortex there are differences in rostral and caudal inhibitory circuits, which are thought to cause spatial variation in odor processing (Large et al., 2018). Following optogenetic activation of GABAergic interneurons along the rostral-caudal axis, pyramidal cells were shown to be inhibited by caudal stimulation whilst interneurons are strongly inhibited by rostral stimulation. These subtle differences in neural circuitry along the rostro caudal axis of the anterior piriform cortex further emphasize its anatomical complexity.

The endopiriform nucleus has a different cellular pattern to piriform cortex proper. It consists of multipolar cells with broad connections to piriform cortex, thalamic regions and orbitofrontal cortex (Behan and Haberly, 1999; Ekstrand et al., 2001). These cells are considered to be important in providing feedback inhibition (Bekkers and Suzuki, 2013). Interestingly multipolar cells have been shown to lie within the dorsal and ventral claustrum of both humans and non-human primates (Baizer et al., 2014; Hinova-Palova et al., 2014). The ventral claustrum in humans consists of projection neurons with spiny dendrites and local interneurons with non-spiny smooth dendrites with the majority of neurons being glutamatergic which facilitate bidirectional communication with the prefrontal cortex (Druga, 2014). These findings further support the equivalence between endopiriform nucleus in rats and the ventral claustrum in humans.

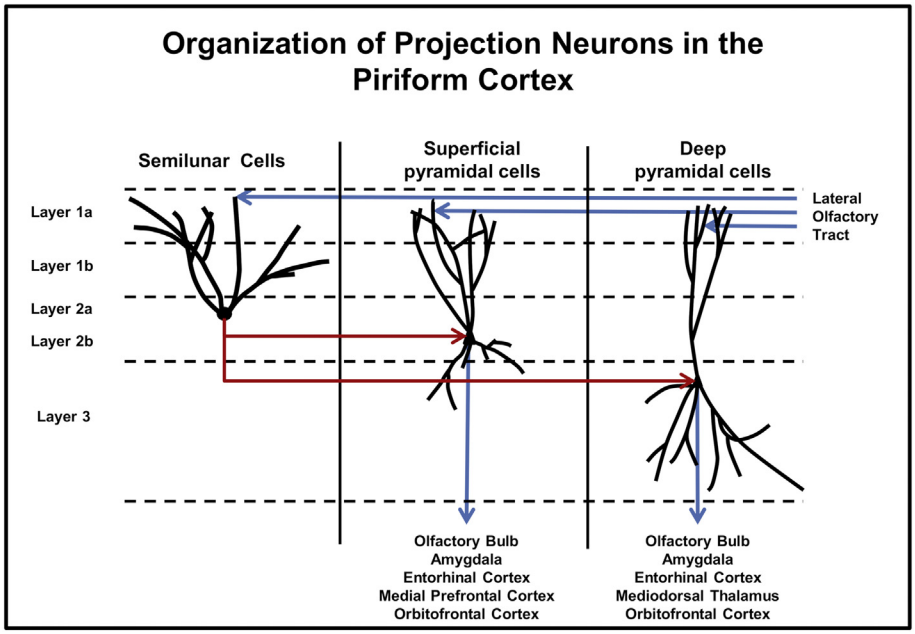

Fig. 2. Organization of Projection Neurons in the Piriform Cortex. Adapted from (Klingler, 2017).

4. Anatomical methods to reveal piriform cortex connectivity

Neuronal tracing studies are the basis of our current understanding of the cellular connectivity of the piriform cortex. Anterograde tracing defines axonal projections from their source (soma) to their termination point (synapse) whilst retrograde tracing traces axonal projections from their synapse to their axon (Deller et al., 2000). Either molecular (e.g. Cholera toxin subunit B (CTB), Flurogold (FG), Horseradish Peroxidase (HRP)), genetic, viral or synthetic microspheres can be injected into the brain region of interest via iontophoresis, micropipette or microsyringe (Katz et al., 1984; Schofield, 2008). For retrograde axonal labelling transports various substances (e.g. lectins, enzymes, synthetic fluorescent compounds) from the soma to the axon and then cross at the synapse onto the next cell. Viral methods typically carry a florescent tag, and can require several weeks to travel along the axons and express. The connections of the anterior, central and posterior piriform cortex were mapped by utilizing the anterograde molecular tracer *Phaseolus vulgaris* leucoagglutinin (Schwabe et al., 2004). In contrast, the mitral-tufted cell projections of the olfactory bulb to the piriform cortex were mapped using different coloured viral tracers (Ghosh et al., 2011). To observe connection of individual cells rather than a cell population, another anterograde molecular tracer biotinylated dextran amine (BDA) can be used in vivo, for example with intracellular injection to cells of the posterior piriform cortex (Johnson et al., 2000). More recently, Schwarz in 2015 utilized canine adenovirus – Cre recombinase (Cav-Cre) and fluorescent microspheres in the anterior piriform, layer 1a and b (Schwarz et al., 2015).

To produce images of neurons labelled in this way entails further technical steps. First, the brain is sectioned conventionally in the coronal plane (for example (Ghosh et al., 2011; Schwabe et al., 2004)) or alternatively at an angle 45° to the sagittal to reduce the number of sections (Johnson et al., 2000) with 60-80 μm section thickness. Labelled neurons can be detected by immunohistochemistry and observed under brightfield microscope (Schwabe et al., 2004) or under fluorescence microscope when using fluorescent proteins(Schwarz et al., 2015). Their 3D course can then be determined by manual or semi-automated tracing (e.g Ghosh et al. (2011)). While fully-automated methods are available for neuron tracing (Peng et al., 2011; Rodriguez et al., 2009) they are limited by a lack of precision due to complex neuron morphology.

4.1. Neuronal connectivity of the piriform cortex

From the olfactory bulb, mitral cells are the predominant input to the piriform cortex. Tufted cells also contribute but to a lesser extent (Neville and Haberly, 2004). The glomeruli in the olfactory bulb project to a wide region of the piriform cortex and synapse with pyramidal cells there (Ghosh et al., 2011; Ojima et al., 1984). Each individual pyramidal cell receives input from an apparently random selection of glomeruli. This allows cells to perform pattern recognition and encode specific features of odor combinations (Davison and Ehlers, 2011). Further inputs to the piriform include the anterior olfactory nucleus and association fibers from all other olfactory cortical regions, as well as commissural fiber projections from the contralateral piriform cortex (Wilson, 1997).

There are also several different neuromodulatory inputs the piriform cortex receives. These include dopaminergic modulation from the ventral tegmental area (Löscher and Ebert, 1996; Shipley and Reyes, 1991) as well as cholinergic modulation from the horizontal limb of the diagonal band and noradrenergic input from the locus coeruleus (Bouret and Sara, 2003). It also been reported serotonin modulation from the raphe nuclei activates inhibitory GABAergic interneurons in the piriform cortex (Pau et al., 2013). In the anterior piriform cortex, the main source of contralateral inputs is the contralateral pars lateralis of the anterior olfactory nucleus, which receives direct projections from the olfactory bulb (Luskin and Price, 1983).

The piriform cortex directly projects to both cortical and subcortical regions broadly feeding into several large scale networks (Neville and Haberly, 2004). These networks include the limbic system, orbitofrontal-thalamic circuit, the fronto-temporal cortical network and the semantic network. Fig. 3 displays the piriform cortex's involvement in networks associated with focal epilepsy.

The strong limbic outputs of the piriform cortex to the entorhinal cortex and amygdala are well established (Johnson et al., 2000; Kajiwara et al., 2007; Krettek and Price, 1977). Limbic processing of olfactory stimuli plays a key role in emotion, memory as well as social behaviour (Chu and Downes, 2002). This process can manifest during the recollection of a memory associated with a specific smell. Amygdala activation is known to occur during exposure to various smells whilst the hippocampus and entorhinal cortex activate during odor classification (Kjelvik et al., 2012; Royet et al., 2003; Winston et al., 2005).

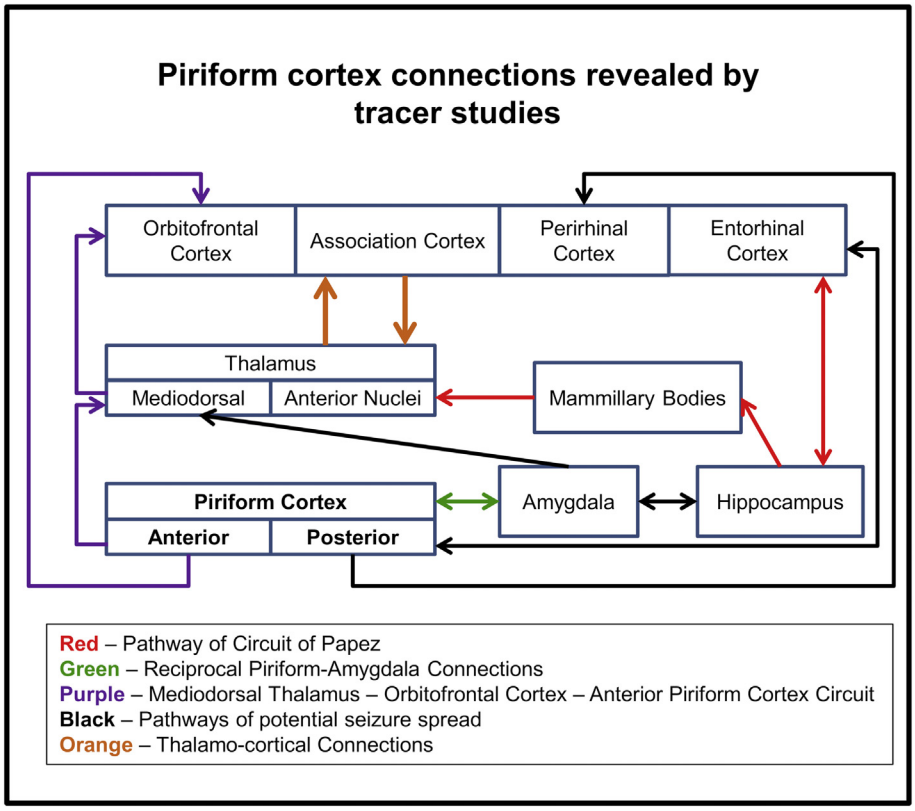

Fig. 3. Piriform cortex connections revealed by tracer studies. Adapted from (Young et al., 2018).

These activations further reflect the piriform cortex's association with emotion and memory.

Piriform cortex connections into the mediodorsal thalamus are considered to be of great importance in olfactory processing including for odor perception, discrimination, attention and learning (Courtiol and Wilson, 2015). This pathway was initially discovered by observing axonal fiber degeneration of in the mediodorsal thalamus following lesioning of the piriform cortex (Powell et al., 1963). The projections from the piriform cortex to the mediodorsal thalamus are topographically arranged, with the anterior and posterior subdivisions of the piriform cortex projecting to the central and medial subdivisions of the mediodorsal thalamus, respectively (Bay and Cavdar, 2013; Cornwall and Phillipson, 1988; Powell et al., 1963; Price, 1985). The endopiriform nucleus projects to the central and medial subdivisions of the mediodorsal thalamus whilst also receiving return projections from the central subdivision (Bay and Cavdar, 2013; Cornwall and Phillipson, 1988). These projections are probably excitatory, having both small and large axonal presynaptic terminals, although this is not fully understood (Kuroda et al., 1992).

The piriform displays frontal lobe connections to the orbitofrontal cortex both directly and also indirectly via the mediodorsal thalamus (Carmichael et al., 1994; Kuroda et al., 1992; Russchen et al., 1987). The orbitofrontal cortex is involved in identifying odors as well as anticipating the onset of olfactory stimuli (Gottfried and Zelano, 2011). It also plays a role in integrating olfactory information, emotion and reward feedback (Kringelbach and Rolls Neville and Haberly, 2004). The mediodorsal nucleus of the thalamus provides an indirect pathway between piriform cortex and the orbitofrontal cortex and is involved in olfactory attention and flavour perception (Tham et al., 2011). The connectivity between all three regions is modulated during olfactory learning and by olfactory attention (Cohen et al., 2015; Plailly et al., 2008).

Downstream connections of the piriform cortex are to the anterior insula via the orbitofrontal cortex and amygdala (Jakab et al., 2011; Mufson et al., 1981). The anterior insula is essential to the processing of olfaction and taste (Veldhuizen and Small, 2011). Furthermore, the anterior insula is also connected to the inferior frontal gyrus which is part of the semantic network (Jakab et al., 2011). The semantic network is important for naming of odors and involves connection to the fusiform gyrus and posterior temporal regions (Savic and Berglund, 2004; Zelano et al., 2009).

5. Macroscopic anatomical imaging of the piriform cortex

There have been various imaging methods applied to analyse the macroscopic anatomical changes of the piriform cortex in epilepsy. These include magnetic resonance (MR) volumetric analysis, diffusion weighted MRI and nuclear medicine methods. The following section considers the approach and protocols for these imaging techniques and how they are best tailored to evaluate the piriform cortex.

5.1. MRI volumetry of the piriform

Measuring the volume of the piriform cortex in vivo is a critical step to assess the impact of disease on this brain region. MRI volumetric analysis has been conducted in two human studies. Gonçalves Pereira et al. (2005) measured atrophy of the piriform cortex in drug-refractory temporal lobe epilepsy whilst Galovic et al. (2019) related the extent of piriform cortex resection to the outcomes of epilepsy surgery with anterior temporal lobectomy (Galovic et al., 2019; Gonçalves Pereira et al., 2005). Both studies performed T1-weighted acquisition by magnetization-prepared rapid acquisition gradient echo sequence (MPRAGE) as detailed in Table 1.

In comparison, many studies have performed high quality in vivo volumetric analysis of the nearby hippocampus, at a range of MRI field strengths and spatial resolutions, for example (Bernasconi et al., 2003; Briellmann et al., 2000). The only major difference is that the usual recommend angle for hippocampal imaging, perpendicular to its long

Table 1
T1-weighted MRI sequence acquisition parameters used for piriform cortex imaging.

Study	Gonçalves Pereira et al. (2005) Piriform imaging	Galovic et al. (2019)* Piriform imaging	Kulaga-Yoskovitz et al. (2015) Hippocampal imaging
Field	1.5T	3T	3T
Sequence	MPRAGE	FSPGR	MPRAGE
Head Coil	Single channel	?	32 channel
TR	10 ms	6.6 ms	2300 ms
TE	4 ms	2.8 ms	2.98 ms
Slice Thickness	2.0 mm	1.1 mm	0.6 mm
Voxel size in-plane	0.98 × 1.30 mm		0.6 × 0.6 mm
Inversion time	250 ms		900 ms
Flip Angle	12°		9

TR = repetition time, TE = echo time, * Galovic (2019) 'derivation' cohort.

axis, is less suitable for piriform cortex imaging. These studies may provide insight into how the piriform cortex could be improved. The multi-contrast submillimetric 3T hippocampal subfield segmentation described in Kulaga-Yoskovitz et al. (2015) may assist in accurately identifying the subdivsions of the piriform cortex in humans (Kulaga-Yoskovitz et al., 2015). The hippocampus has also been imaged at 7T for the assessment of subdivision volumetry in epilepsy (Santyr et al., 2017), a technique which may also contribute to identifying abnormalities in piriform cortex subdivisions. Such studies are yet to be performed however.

5.1.1. Piriform cortex manual segmentation in humans

In both studies, manual tracing was used to outline the piriform cortex and cortical amygdala together, on coronal T1-weighted images. However, Gonçalves Pereira et al. (2005) notably did not include the frontal lobe portion of the piriform cortex. Galovic et al. (2019) based their method on the earlier study, however they did include the frontal lobe portion. They defined the frontal portion as extending from the tip of the endorhinal sulcus, going medially to the olfactory tubercle and limited laterally by the olfactory tubercle. Furthermore, a percentage of the distance from the endorhinal sulcus to the olfactory tubercle (50–75%) was also included as part of the frontal portion of the piriform cortex (Vaughan and Jackson, 2014). The temporal lobe portion of the piriform cortex extends posteriorly towards the amygdala, occupying gradually 25%, 50%, 75% and then 100% of the distance to the fundus of the sulcus semianularis. The caudal end of the amygdala and the appearance of the interpeduncular cistern and the mammillary bodies are used as a landmark for the hippocampal head where the final slice is outlined. A 3D reconstruction of this outlining method is shown in Fig. 4.

Whilst there are several software packages for automated parcellation of the hippocampus (for example, Hipposeg) (Winston et al., 2013), amygdala and entorhinal cortex (such as Geodesic Information Flows) (Cardoso et al., 2015) were used in Galovic et al. (2019). FreeSurfer and CLASP are other common automated parcellation software used in humans (Kim et al., 2005; Schmidt et al., 2018). However there is no current parcellation algorithm for the piriform cortex. Future studies that endeavour to automate this process will be very beneficial for the advanced assessment of epilepsy.

Notably, both studies utilized a coronal plane for manually tracing the piriform cortex. Vaughan and Jackson (2014) describe an oblique-axial orientation (approximately +20° relative to the anterior commissure-posterior commissure axis) termed the "piriform axis" (Fig. 5). This axis allows for the relationship between the piriform cortex, amygdala and hippocampus to be easily observed. Furthermore, it provides a perpendicular plane to the U-shaped cross-section at the anterior part of the piriform cortex, reducing partial voluming and the required number of slices in this region. Voxel-based morphometry (VBM (Ashburner and Friston, 2000)) is a method used by Galvoic et al. (2019) to look for brain-wide changes in grey matter volume, and this gave the initial signal in that patient group that the fraction resected of the piriform was of interest. However, direct measurement of piriform cortex volume would be generally considered a more accurate and sensitive measure, and to be preferred over a VBM analysis.

5.2. T2-weighted and diffusion imaging

Various MRI sequences have been used to assess neurodegeneration at the limbic structures after status epilepticus in animal models, including at the piriform cortex (Eidt et al., 2004; Roch et al., 2002; Wall et al., 2000). Wall et al. (2000) utilized diffusion weighted imaging ($b = 1228 s/mm^2$) and a multi-echo T2-weighted sequence to determine local neurodegenerative changes following status epilepticus (Fig. 6). The piriform cortex was estimated by drawing a region of interest (including entorhinal and perirhinal cortices) based upon its location in the rat brain stereotaxic atlas (Paxinos and Watson, 1998). In contrast, Roch et al. (2002) utilized a 4.7T field and a section thickness of 1 mm greatly increasing the resolution for T2-weighted imaging (Table 2).

For diffusion weighted imaging, Eidt et al. (2004) also performed a similar study to Wall et al. (2000) however they utilized an approximation of q-space imaging to more accurately acquire diffusion weighted images of the piriform cortex in a post-status epileptic rat model (Table 3). The resolution of diffusion weighted images in this study was also far greater due to the 3T field and q-space imaging allowed for neuronal and glial cells to be distinguished from one another. More recent diffusion weighted imaging studies have utilized fields of 9.4T (Dunn et al., 2009) and 16.4T (Alomair et al., 2015) to yield greater spatial resolution. Alomair et al. (2015) demonstrated the echo-planar imaging diffusion weighted imaging (EPI-DWI) sequence at 16.4T was able to produce images with high spatial and angular resolution (Alomair et al., 2015). This sequence applied to post-status epileptic animal models may allow for more accurate estimations of neurodegenerative alterations of the piriform cortex.

5.3. Other magnetic resonance imaging methods

There are other MR imaging modalities which may be useful in future studies of the piriform cortex in epilepsy. Diffusion-based imaging techniques have been utilized in estimating structure connectivity of the olfactory system. The circuitry of the olfactory system has been typically investigated using anatomical microsurgery dissection (Kavoi and Jameela, 2011), however there have been recent efforts to utilize imaging techniques to visualize the olfactory tracts. Most notably, Skorpil et al. (2011) were able to demonstrate fiber tracking of distal olfactory tracts from diffusion tensor imaging (DTI) (Skorpil et al., 2011). However DTI cannot determine how fibers with complex axonal configurations interact (Tournier et al., 2008). More recently, constrained spherical deconvolution (CSD) has been applied which has improved upon previous anatomical imaging techniques (Milardi et al., 2017). However, even with this technique the proximal part of the olfactory tract could not be reconstructed, possibly due to the thin diameter of fiber bundles.

There have also been recent advanced in ultra-high field MR imaging modalities which allows for imaging at greater field strengths (7T in humans) and can be used to detect anatomical abnormalities due to their increased sensitive compared to conventional MR. It has been recently used in differentiating between subtypes of hippocampal sclerosis using a 3D T2-weighted turbo spin echo sequence at 7T (Gillmann et al., 2018) and has shown to improve visualization of the amygdalo-hippocampal border compared to 3T (T1-weighted imaging) (Derix et al., 2014).

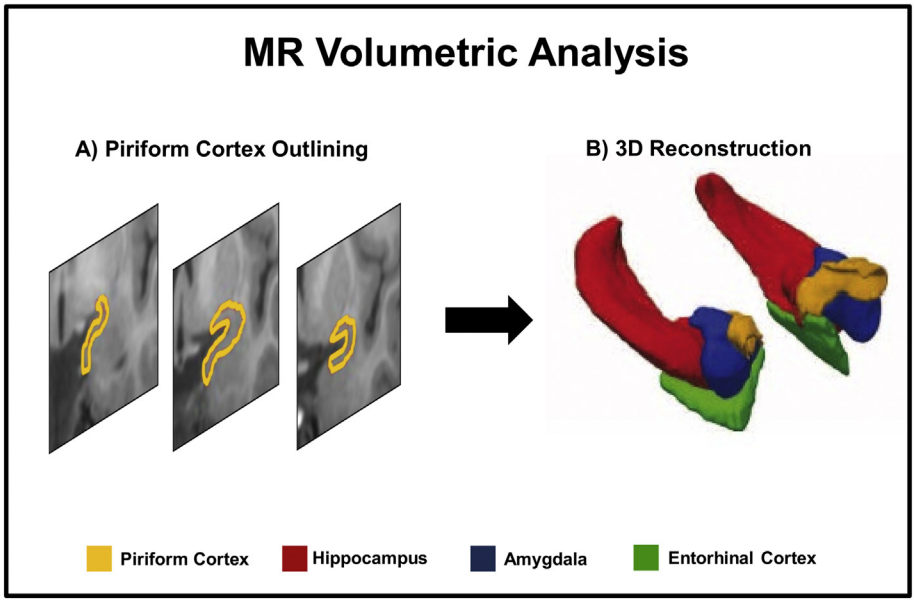

Fig. 4. MR Volumetric Analysis of Piriform Cortex in Galovic (2019). A) Piriform cortex outlining at three different stages of manual tracing on T1-weighted coronal images. B) 3D reconstruction of the piriform cortex and its anatomical relationship with the hippocampus, amygdala and entorhinal cortex. Adapted from Galovic et al. (2019).

5.4. Anatomical nuclear medicine techniques

Nuclear medicine techniques have also been utilized in anatomical imaging of the piriform cortex in epilepsy. These techniques are primarily used to reveal the nature of brain function, rather than anatomical detail. Positron emission topography (PET) imaging detects gamma rays emitted by radioactive tracers injected into the body to detect in metabolic processes (Vaquero and Kinahan, 2015). Laufs et al. (2011) utilized PET (FMZ tracer) and functional MRI to demonstrate the piriform cortex as a common node of the focal epilepsy network in humans (Laufs et al., 2011). Other studies of temporal lobe epilepsy patients using PET imaging have only shown changes in hippocampus and amygdala however these studies utilized different tracers (FDG and ^{11}C-PBR28) which may account for these conflicting findings (Hirvonen et al., 2011; Leiva-Salinas et al., 2017).

Another nuclear medicine technique used to study the piriform cortex in epilepsy is autoradiography. Autoradiography uses X-ray film to visualize molecules that have been radioactively labelled. Local cerebral blood flow can be measured by injecting autoradiographic diffusible tracers into rodents and evaluating changes in concentration of the labelled tissue (Sakurada et al., 1978). This method has been previously applied to measure local cerebral blood flow in limbic structures, including the piriform cortex, in the genetic absence epilepsy rat model (GAERS) during kindling (Carçak et al., 2009).

6. Piriform cortex imaging findings associated with epilepsy

The various imaging studies conducted on the piriform cortex in epilepsy have provided insight into its morphological changes and potential early involvement in focal epilepsies as well as its possible

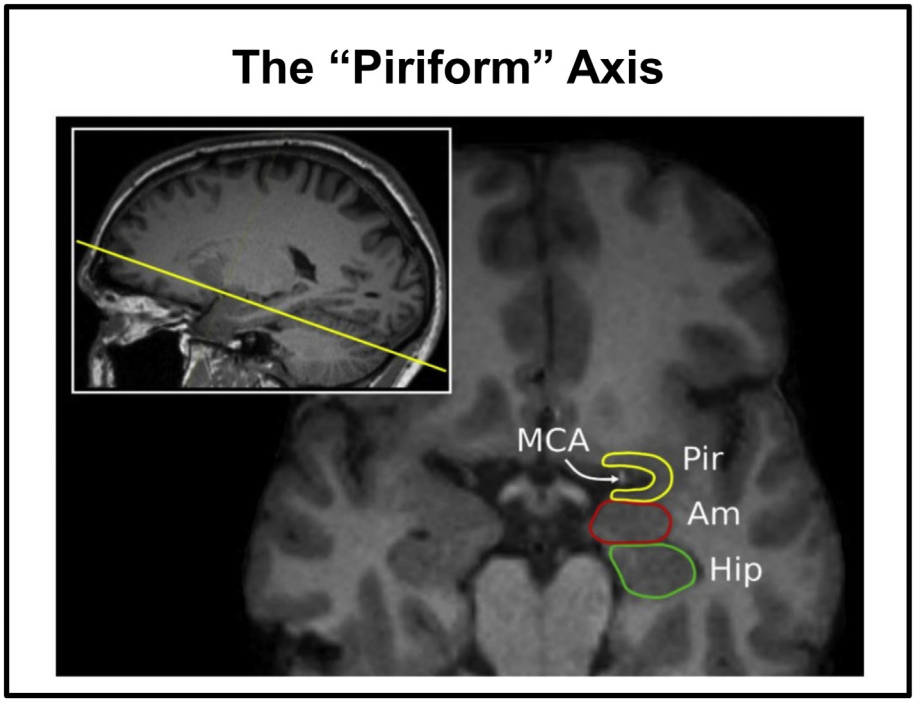

Fig. 5. T1-weighted MPRAGE image of a healthy adult male, displayed in para-sagittal (small image) and oblique-axial orientation (large image), approximately +20° relative to the anterior commissure-posterior commissure axis. Pir = piriform cortex, Am = amygdala, Hip = hippocampus,. The arrow indicates the location of the middle cerebral artery (MCA) within the endorhinal sulcus. Fig. 5 reproduced from Vaughan and Jackson (2014).

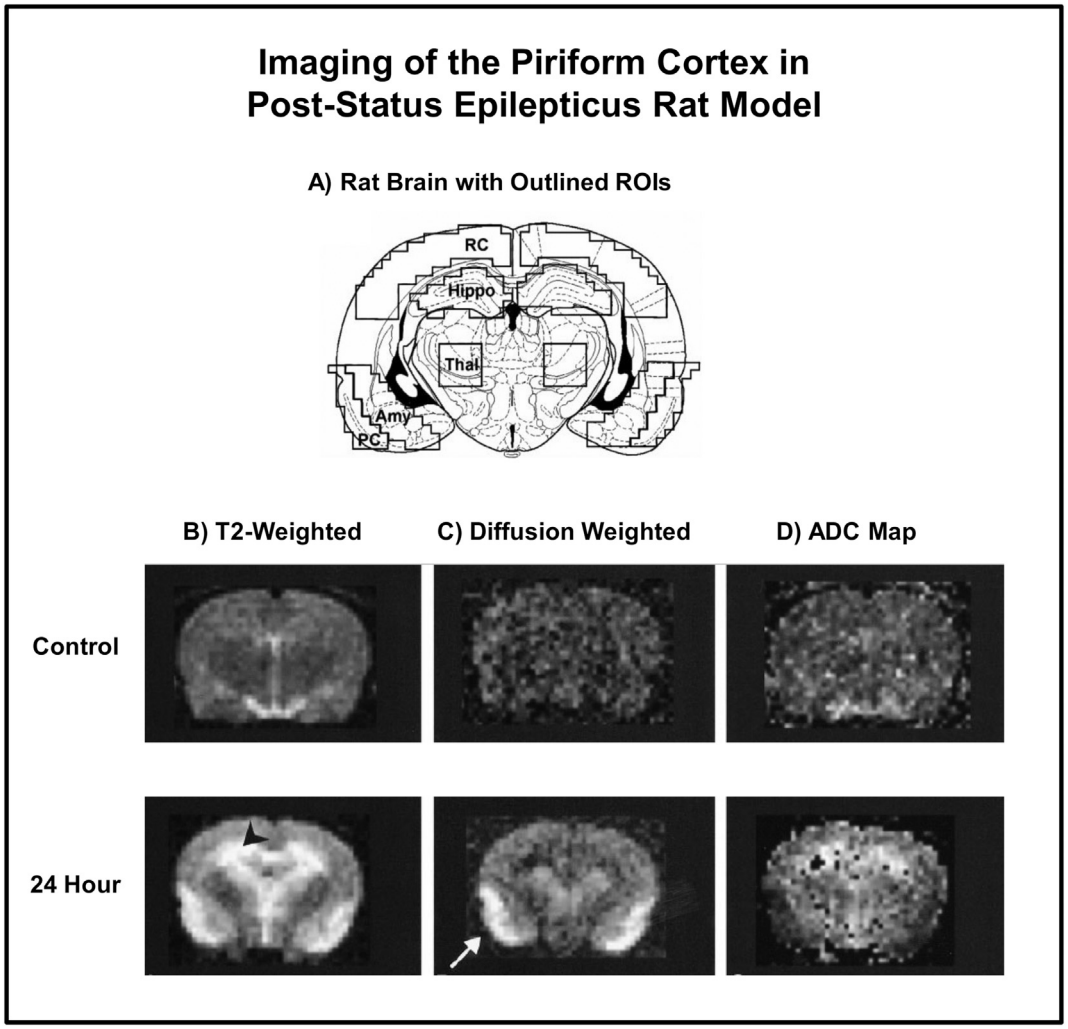

Fig. 6. Imaging of piriform cortex in status epilepticus rat model (pilocarpine). A) Schematic of rat brain with regions of interest (ROIs) for retrosplenial cortex (RC), hippocampus (Hippo), thalamus (Thal), amygdala (Amy), piriform cortex (PC). B) T2-weighted image (b = 0 s/cm^2). C) Diffusion weighted image (b = 1228 s/cm^2). D) Apparent diffusion coefficient maps. Top row = images for control rat. Bottom row = images following status epilepticus induced by pilocarpine after 24 h. Black arrow = hippocampus. White arrow = piriform cortex. Adapted from (Wall et al., 2000).

Table 2
T2-weighted imaging parameters.

Study	Wall et al. (2000)	Roch et al. (2002)
Sequence	Multi-echo T2-weighted	T2-Weighted, spin-echo fast imaging method
Field	1.5T	4.7T
Section Thickness	2 mm	1 mm
Matrix	128 × 128	256 × 256 (FOV = 60 mm)
TR	2000 ms	3800 ms
TE	20 ms	80 ms
Echoes	16	

TR = repetition time, TE = echo time, FOV = Field of View.

Table 3
Diffusion Weighted Imaging (DWI) Parameters.

Study	Wall et al. (2000)	Eidt et al. (2004)	Alomair et al. (2015)
Sequence	DWI	DWI	EPI-DWI
Field	1.5	3T	16.4T
Section Thickness	2 mm	2 mm	0.6 mm
Matrix	128 × 128	128 × 128	128 × 64
TR	2200 ms	3200 ms	6000 ms
TE	111 ms	100 ms	13.97 ms
b value	0, 1228 s/mm^2	0–30,000 s/mm^2	3000 s/mm^2
Echoes		50	

TR = repetition time, TE = echo time, b = constant derived from magnitude of diffusion gradients.

contributions to absence epilepsy. The following section describes the current findings of direct anatomical changes to the piriform cortex in epilepsy, epileptic lesions of the piriform cortex and neurodegeneration of the piriform cortex following status epilepticus.

6.1. Epileptic lesions of the piriform cortex

Various types of lesions have been reported to impact the piriform cortex and have been associated with olfactory auras. Olfactory experiences require the coordination of multiple brain regions associated with the olfactory network (Baars, 2013; Keller, 2011), which includes the piriform cortex due to its central role in olfactory identification (Zatorre et al., 1992). The most common type of lesions impacting the piriform cortex are tumors whilst mesial temporal sclerosis is rarer (Acharya et al., 1998). Acharya et al. (1998) reported 10 out 13 patients with olfactory aura were the result of tumor revealed via T1-weighted MRI. These tumors were predominantly low grade astrocytoma which are associated with epileptogenesis in focal epilepsy (Rudà et al., 2012). A case of ganglioglioma and dysembryplastic neuroepithelial tumors were also reported in Acharya et al. (1998). Low-grade astrocytomas were also described by Chen et al. (2003) as the most common type of

tumor involving the piriform cortex via T1-weighted and T2-weighted MRI (Chen et al., 2003). They also reported cases of anaplastic astrocytoma and glioblastoma multiforme tumors, all located in the right mesial temporal lobe. Whilst Acharya et al. (1998) suggest the amygdala as the most likely symptomatogenic zone of olfactory auras as a result of tumors, Chen et al. (2003) described cases of tumors resulting in olfactory auras without the involvement of the amygdala suggesting it is not critical to olfactory aura manifestation compared to the piriform cortex.

Other rare lesions affecting the piriform cortex include a case of arteriovenous malformation reported in Chen et al. (2003) and an aneurysm of the middle cerebral artery described by Mizobuchi et al. (1999). A woman developed new onset focal seizures as well as strong olfactory hallucinations as a result of an aneurysm in the middle cerebral artery (Mizobuchi et al., 1999). This was revealed by both CT angiogram reconstructions of the middle cerebral artery as well as T1-weighted MR imaging. Following neurosurgical clipping of the aneurysm, she became seizure free suggesting extrinsic compression of the piriform cortex may trigger seizure activity.

6.2. Piriform cortex in chronic epilepsy

Volumetric analysis of the piriform cortex has revealed significant anatomical changes in temporal lobe epilepsy (Gonçalves Pereira et al., 2005). Reduction in volume of the temporal piriform cortex was found on the same side as the epileptic focus with the effect reportedly greater with right-sided epilepsy. The degree of piriform atrophy was correlated with ipsilateral volume loss at the hippocampus, suggesting a common mechanism of neuronal loss in these regions. Furthermore, atrophy in the hippocampus, entorhinal cortex and amygdala suggest the atrophy of the piriform cortex may be the result of piriform cortex engagement with temporal lobe epilepsy networks (Vaughan and Jackson, 2014).

The critical involvement of the piriform cortex in temporal lobe epilepsy compared to other limbic structures is further revealed in the recent Galovic et al. (2019) findings (Galovic et al., 2019). Resection of at least half the piriform cortex increased the odds of seizure freedom by a factor of 16 whilst overall resection volumes of the hippocampus, amygdala and entorhinal cortex were not significantly associated with seizure outcomes. However it was not reported what percentage of frontal and temporal portions of the piriform cortex were resected and whether these correlate with seizure freedom. Given the possible localization of the area tempestas deep to the frontal portion of the piriform cortex, segmentation of the piriform cortex subdivisions in human imaging data would be a worthy endeavour for future studies.

In contrast to temporal lobe epilepsy findings, one study of frontal lobe epilepsy has demonstrated bilateral increases in volume of the piriform cortex and amygdala compared to control with no atrophy present (Centeno et al., 2014). It remains unclear why there is an increase in grey matter volume.

PET imaging in conjunction with functional MRI has demonstrated the piriform cortex, specifically the frontal portion, as common region of interest in patients with focal epilepsy (Laufs et al., 2011). This occurred ipsilateral to the presumed cortical focus and further emphasizes the importance of developing methods to segment the piriform cortex into its frontal and temporal portions in future anatomical imaging studies. There is also preliminary evidence of changes in the piriform cortex in absence epilepsy via local cerebral blood flow changes detected by quantitative autoradiography (Carçak et al., 2009). During kindling in GAERS rat model, there was an increase in local cerebral blood flow in the somatosensory cortex, ventrobasal thalamus, anterior thalamic nuclei, hypothalamus, subthalmic nucleus, entorhinal cortex, perirhinal cortex, amygdala, CA2 region of the hippocampus, substantia nigra and the piriform cortex. These findings allude to a possible relationship between thalamo-cortical networks and limbic structures in absence epilepsy (Carçak et al., 2009).

6.2.1. Post-status epilepticus animal models

Piriform cortex injury is seen after status epilepticus induced by the chemoconvulsants kainic acid and pilocarpine in rodents which results in spontaneous recurrent seizures being developed after 12 weeks (Van Nieuwenhuyse et al., 2015). These post-status epilepticus models are considered to be animal models of chronic temporal lobe epilepsy (Curia et al., 2008; Van Nieuwenhuyse et al., 2015). These models produce observable tissue damage and lesions in the hippocampus, amygdala, piriform cortex and other limbic regions (Sharma et al., 2007). Serial MRI has demonstrated that the piriform cortex and entorhinal cortex undergo the earliest changes following status epilepticus, highlighting their susceptibility to neuronal injury (Wall et al., 2000). There was a decrease in apparent diffusion coefficient in the piriform cortex and amygdala at 12 h which correlated with an increase in neuronal degeneration (layer II and III of piriform cortex) which remained low at 24 h. Again using the pilocarpine post-status epilepticus rat model, Roch et al. (2002) performed a similar study however they extended the observation of neurodegeneration to 9 weeks. Neurodegeneration was shown to persist for up to 2 weeks in layer III of the piriform cortex following status epilepticus, demonstrating long term pathological changes (Roch et al., 2002). Furthermore, approximation q-spacing imaging of the piriform cortex in the same animal model also demonstrated neurodegeneration and an increase in glial cell population (Eidt et al., 2004).

However, imaging findings using the pilocarpine rat model may differ from other post-status epilepticus model findings, as Wang et al. (1996) demonstrate a faster neuronal death in the hippocampus in the kainic acid model compared to pilocarpine (Wang et al., 1996). Piriform cortex has shown to display enhanced neurogenesis and synaptic reorganization following kainic acid induced status epilepticus (Sakurai et al., 2018), however there are also conflicting reports of kainic acid induced status epilepticus not displaying any damage in diffusion weighted imaging findings (Yi-Hua et al., 2007). Therefore, the early damage observed in the piriform cortex post-status epilepticus may be dependent upon the chemoconvulsant used to induce status epilepticus.

6.2.2. Human cases of status epilepticus

Early anatomical changes in piriform cortex following status epilepticus has also been observed in humans (Legriel et al., 2010). This has been observed in three human cases of status epilepticus (neuroleptic malignant syndrome, carcinomatous meningitis and an unknown case) (Fujikawa et al., 2000). Most notably, none of these people had a history of epilepsy. These cases can be considered to be new-onset prolonged focal status epilepticus with altered awareness and motor manifestation, in contrast to epilepsia partialis continua or non-convulsive generalized status epilepticus. Status epilepticus occurred on EEG for 9 to 72 h with death occurring between 11 and 27 days following the commencement of status epilepticus. It was revealed in post-mortem that there was greatest neuronal loss in the piriform cortex, amygdala and hippocampus, with glutamate excitotoxicity hypothesized as the underlying cause for injury.

The influence of glutamatergic excitotoxicity of the piriform cortex has also been demonstrated through studies using the neurotoxin domoic acid. Domoic acid and kainic acid activate glutamate receptors in a similar fashion (Hampson and Manalo, 1998). In preclinical work, systemic injections of domoic acid induce status epilepticus (Olga, 2008). The most significant early changes occurred in the olfactory bulb and endopiriform nucleus (Tiedeken et al., 2013). There are also cases of domoic acid causing neuronal toxicity in human piriform cortex post-status epilepticus. In 1987, 14 people ate mussels contaminated with domoic acid resulting in them displaying seizures and impaired consciousness (Teitelbaum et al., 1990). 4 people died as a result and all demonstrated significant damage to the hippocampus whilst also exhibiting damage to amygdala, piriform cortex, claustrum and mediodorsal thalamus. Similar findings were also present an 84 year old man who survived. Domoic acid toxicity resulted in him developing

temporal lobe epilepsy (Cendes et al., 1995). After his death, there was complete neuronal loss in CA1 and CA3 however there was only mild to moderate neuronal loss in amygdala, piriform cortex. These findings in domoic acid neuronal toxicity are akin to those produced by kainic acid rats (Sperk et al., 1983) as well as the cases described in Fujikawa et al. (2000) (Fujikawa et al., 2000). Both the Fujikawa et al. (2000) and Teitelbaum et al. (1990) findings demonstrate status epilepticus induced neuronal damage and resulting reorganization of the brain were the underlying cause of seizures with excitotoxic injury to the limbic structures, including the piriform cortex, playing a potential role in epileptogenesis.

7. Future directions and conclusions

Macroscopic anatomical imaging findings demonstrate significant anatomical changes in the piriform cortex and neighbouring regions, specifically in focal epilepsy. Microscopic imaging methods, on the other hand, reveal the broad connections the piriform cortex displays to various limbic structures and cortical regions making it well-placed for seizure propagation. Whilst there have been recent improvements in volumetric analysis of the piriform cortex, future imaging studies should endeavour to improve methods of piriform cortex subdivision, as it is clearly not a homogeneous structure, and this anatomical detail can have a great impact on the nature of dysfunction that can be caused through localized lesions. Imaging techniques which allow for quantification of local pathological changes within the piriform cortex should also be applied in future studies of epilepsy in humans. Finally, the preliminary evidence of piriform cortex abnormality in absence epilepsy warrants further investigation through both imaging and electrophysiology studies to better understand the role of piriform cortex in the generalized epilepsies.

Declaration of Competing Interest

None.

Acknowledgments

The Florey Institute of Neuroscience and Mental Health acknowledges the strong support from the Victorian Government and in particular the funding from the Operational Infrastructure Support Grant. This study was supported by the National Health and Medical Research Council of Australia (NHMRC Project Grant 1091593). James C Young acknowledges that they have been supported through an Australian Government Research Training Program Scholarship.

References

Neville, K.R.A., Haberly, L.B.A., 2004. Olfactory Cortex. Oxford University Press, New York.
Pau, E., ePuig, M.V., Francesc, E., 2013. Serotonin modulation of cortical neurons and networks. Frontiers in Integrative Neuroscience, Vol 7 (2013).
Kajiwara, R., Tominaga, T., Takashima, I., 2007. Olfactory information converges in the amygdaloid cortex via the piriform and entorhinal cortices: observations in the guinea pig isolated whole-brain preparation. European Journal of Neuroscience 25, 3648–3658.
Acharya, V., Acharya, J., Lüders, H., 1998. Olfactory epileptic auras. Neurology 51, 56–61.
Allison, A.C., 1954. The secondary olfactory areas in the human brain. J. Anat. 88 (481-488.482).
Alomair, O.I., Brereton, I.M., Smith, M.T., Galloway, G.J., Kurniawan, N.D., 2015. In vivo high angular resolution diffusion-weighted imaging of mouse brain at 16.4 Tesla. PLoS One 10, e0130133.
Ashburner, J., Friston, K.J., 2000. Voxel-based morphometry—the methods. NeuroImage 11, 805–821.
Baars, B.J., 2013. Multiple Sources of Conscious Odor Integration and Propagation in Olfactory Cortex.
Baizer, J.S., Sherwood, C.C., Noonan, M., Hof, P.R., 2014. Comparative organization of the claustrum: what does structure tell us about function? Front. Syst. Neurosci. 8, 117.
Barnes, D.C., Hofacer, R.D., Zaman, A.R., Rennaker, R.L., Wilson, D.A., 2008. Olfactory perceptual stability and discrimination. Nat. Neurosci. 11, 1378–1380.
Bay, H.H., Cavdar, S., 2013. Regional Connections of the Mediodorsal Thalamic Nucleus in the Rat. Imperial College Press, pp. 201.
Behan, M., Haberly, L.B., 1999. Intrinsic and efferent connections of the endopiriform nucleus in rat. J. Comp. Neurol. 408, 532–548.
Bekkers, J.M., Suzuki, N., 2013. Review: neurons and circuits for odor processing in the piriform cortex. Trends Neurosci. 36, 429–438.
Bernasconi, N., Bernasconi, A., Caramanos, Z., Antel, S.B., Andermann, F., Arnold, D.L., 2003. Mesial temporal damage in temporal lobe epilepsy: a volumetric MRI study of the hippocampus, amygdala and parahippocampal region. Brain 126, 462–469.
Bouret, S., Sara, S., 2003. Locus Coeruleus Activation Modulates Firing Rate and Temporal Organization of Odour-Induced Single-Cell Responses in Rat Piriform Cortex.
Brian, N.M., 2014. The claustrum in review. Frontiers in Systems Neuroscience, Vol 8 (2014).
Briellmann, R.S., Berkovic, S.F., Jackson, G.D., 2000. Men may be more vulnerable to seizure-associated brain damage. Neurology 55, 1479–1485.
Carçak, N., Ferrandon, A., Koning, E., Aker, R.G., Ozdemir, O., Onat, F.Y., Nehlig, A., 2009. Effect of stage 2 kindling on local cerebral blood flow rates in rats with genetic absence epilepsy. Epilepsia 50, 33–43.
Cardoso, M.J., Modat, M., Wolz, R., Melbourne, A., Cash, D., Rueckert, D., Ourselin, S., 2015. Geodesic information flows: spatially-variant graphs and their application to segmentation and fusion. IEEE Trans. Med. Imaging 1976.
Carmichael, S.T., Clugnet, M.C., Price, J.L., 1994. Central Olfactory Connections in the Macaque Monkey. pp. 403–434.
Cendes, F., Andermann, F., Carpenter, S., Zatorre, R.J., Cashman, N.R., 1995. Temporal lobe epilepsy caused by domoic acid intoxication: evidence for glutamate receptor-mediated excitotoxicity in humans. Ann. Neurol. 37, 123–126.
Centeno, M., Vollmar, C., Stretton, J., Symms, M.R., Thompson, P.J., Richardson, M.P., O'Muircheartaigh, J., Duncan, J.S., Koepp, M.J., 2014. Structural changes in the temporal lobe and piriform cortex in frontal lobe epilepsy. Epilepsy Res. 108, 978–981.
Chen, C., Shih, Y.-H., Yen, D.-J., Lirng, J.-F., Guo, Y.-C., Yu, H.-Y., Yiu, C.-H., 2003. Olfactory auras in patients with temporal lobe epilepsy. Epilepsia 44, 257–260 Series 4.
Chu, S., Downes, J.J., 2002. Proust nose best: odors are better cues of autobiographical memory. Mem. Cogn. 30, 511–518.
Cohen, Y., Putrino, D., Wilson, D.A., 2015. Dynamic cortical lateralization during olfactory discrimination learning. J. Physiol. 1701.
Cornwall, J., Phillipson, O.T., 1988. Afferent projections to the dorsal thalamus of the rat as shown by retrograde lectin transport—I. The mediodorsal nucleus. Neuroscience 24, 1035–1049.
Courtiol, E., Wilson, D.A., 2015. The olfactory thalamus: unanswered questions about the role of the mediodorsal thalamic nucleus in olfaction. Frontiers In Neural Circuits 9, 49.
Curia, G., Longo, D., Biagini, G., Jones, R.S.G., Avoli, M., 2008. Invited review: the pilocarpine model of temporal lobe epilepsy. J. Neurosci. Methods 172, 143–157.
Davison, I., Ehlers, M., 2011. Neural Circuit Mechanisms for Pattern Detection and Feature Combination in Olfactory Cortex.
Deller, T., Naumann, T., Frotscher, M., 2000. Retrograde and anterograde tracing combined with transmitter identification and electron microscopy. J. Neurosci. Methods 103, 117–126.
Derix, J., Yang, S., Lusebrink, F., Fiederer, L.D.J., Schulze-Bonhage, A., Aertsen, A., Speck, O., Ball, T., 2014. Visualization of the amygdalo-hippocampal border and its structural variability by 7T and 3T magnetic resonance imaging. Hum. Brain Mapp. 4316.
Dillingham, C.M., Jankowski, M.M., Chandra, R., Frost, B.E., O'Mara, S.M., 2017. The claustrum: considerations regarding its anatomy, functions and a programme for research. Brain and Neuroscience Advances 1 (2398212817718962).
Druga, R., 2014. Chapter 2 - the structure and connections of the claustrum. In: Smythies, J.R., Edelstein, L.R., Ramachandran, V.S. (Eds.), The Claustrum. Academic Press, San Diego, pp. 29–84.
Dunn, J.F., Tuor, U.I., Kmech, J., Young, N.A., Henderson, A.K., Jackson, J.C., Valentine, P.A., Teskey, G.C., 2009. Functional brain mapping at 9.4T using a new MRI-compatible electrode chronically implanted in rats. Magn. Reson. Med. 61, 222–228.
Eidt, S., Kendall, E.J., Obenaus, A., 2004. Neuronal and glial cell populations in the piriform cortex distinguished by using an approximation of q-space imaging after status epilepticus. Am. J. Neuroradiol. 25, 1225.
Ekstrand, J.J., Domroese, M.E., Johnson, D.M., Feig, S.L., Knodel, S.M., Behan, M., Haberly, L.B., 2001. A new subdivision of anterior piriform cortex and associated deep nucleus with novel features of interest for olfaction and epilepsy. J. Comp. Neurol. 434, 289–307.
Franks, Kevin M., Russo, Marco J., Sosulski, Dara L., Mulligan, Abigail A., Siegelbaum, Steven A., Axel, R., 2011. Report: recurrent circuitry dynamically shapes the activation of piriform cortex. Neuron 72, 49–56.
Fujikawa, D.G., Itabashi, H.H., Wu, A., Shinmei, S.S., 2000. Status epilepticus–induced neuronal loss in humans without systemic complications or epilepsy. Epilepsia 41, 981–991.
Gale, K., 1988. Progression and generalization of seizure discharge: anatomical and neurochemical substrates. Epilepsia 29 (Suppl. 2), S15–S34.
Galovic, M., Baudracco, I., Wright-Goff, E., Pillajo, G., Nachev, P., Wandschneider, B., Woermann, F., Thompson, P., Baxendale, S., McEvoy, A., Nowell, M., Mancini, M., Vos, S., Winston, P., Sparks, R., Prados, F., Miserocchi, A., de Tisi, J., André Van Graan, L., Koepp, J., 2019. Association of Piriform Cortex Resection With Surgical Outcomes in Patients With Temporal Lobe Epilepsy.
Gerrard, L.B., Tantirigama, M.L.S., Bekkers, J.M., 2018. Pre- and postsynaptic activation of GABAB receptors modulates principal cell excitation in the piriform cortex. Front.

Cell. Neurosci. 12.
Ghosh, S., Larson, S.D., Hefzi, H., Marnoy, Z., Cutforth, T., Dokka, K., Baldwin, K.K., 2011. Sensory maps in the olfactory cortex defined by long-range viral tracing of single neurons. Nature 472, 217–220.
Gillmann, C., Coras, R., Rössler, K., Doerfler, A., Uder, M., Blümcke, I., Bäuerle, T., 2018. Ultra-high field MRI of human hippocampi: morphological and multiparametric differentiation of hippocampal sclerosis subtypes. PLoS One 13, e0196008.
Gonçalves Pereira, P.M., Insausti, R., Artacho-Pérula, E., Salmenperä, T., Kälviäinen, R., Pitkänen, A., 2005. MR volumetric analysis of the piriform cortex and cortical amygdala in drug-refractory temporal lobe epilepsy. Am. J. Neuroradiol. 26, 319–332.
Gottfried, J.A., Zald, D.H., 2005. Review: on the scent of human olfactory orbitofrontal cortex: meta-analysis and comparison to non-human primates. Brain Res. Rev. 50, 287–304.
Gottfried, J.A., Zelano, C., 2011. The value of identity: olfactory notes on orbitofrontal cortex function. Ann. N. Y. Acad. Sci. 1239, 138–148.
Haberly, L.B., 1985. Neuronal circuitry in olfactory cortex: anatomy and functional implications. Chem. Senses 10, 219–238.
Haberly, L.B., Price, J.L., 1978. Association and commissural fiber systems of the olfactory cortex of the rat. I. Systems originating in the piriform cortex and adjacent areas. J. Comp. Neurol. 178, 711.
Hagiwara, A., Pal, S.K., Sato, T.F., Wienisch, M., Murthy, V.N., 2012. Optophysiological analysis of associational circuits in the olfactory cortex. Front. Neural Circuits 6, 18.
Hampson, D.R., Manalo, J.L., 1998. The activation of glutamate receptors by kainic acid and domoic acid. Nat. Toxins 6, 153–158.
Hinova-Palova, D.V., Edelstein, L., Landzhov, B., Minkov, M., Malinova, L., Hristov, S., Denaro, F.J., Alexandrov, A., Kiriakova, T., Brainova, I., Paloff, A., Ovtscharoff, W., 2014. Topographical distribution and morphology of NADPH-diaphorase-stained neurons in the human claustrum. Front. Syst. Neurosci. 8.
Hirvonen, J., Kreisl, W., Fujita, M., Dustin, I., Khan, O., Zhang, Y., Morse, C., Pike, V., Theodore, W., Innis, R., 2011. Increased In Vivo Expression of an Inflammatory Marker in Temporal Lobe Epilepsy.
Jakab, A., Molnar, P., Bogner, P., Monika, B., Berényi, E., 2011. Connectivity-Based Parcellation Reveals Interhemispheric Differences in the Insula.
Johnson, D.M.G., Illig, K.R., Behan, M., Haberly, L.B., 2000. New features of connectivity in piriform cortex visualized by intracellular injection of pyramidal cells suggest that "primary" olfactory cortex functions like "association" cortex in other sensory systems. J. Neurosci. 20, 6974.
Katz, L.C., Burkhalter, A., Dreyer, W.J., 1984. Fluorescent latex microspheres as a retrograde neuronal marker for in vivo and in vitro studies of visual cortex. Nature 310, 498–500.
Kavoi, B.M., Jameela, H., 2011. Comparative morphometry of the olfactory bulb, tract and stria in the human, dog and goat. Morfometría Comparada del Bulbo, Tracto y Estría Olfatoria en el Humano, Perro y Cabra. 29, 939–946.
Keller, A., 2011. Attention and Olfactory Consciousness.
Kim, J.S., Singh, V., Lee, J.K., Lerch, J., Ad-Dab'bagh, Y., MacDonald, D., Lee, J.M., Kim, S.I., Evans, A.C., 2005. Automated 3-D extraction and evaluation of the inner and outer cortical surfaces using a Laplacian map and partial volume effect classification. Neuroimage 27, 210–221.
Kjelvik, G., Evensmoen, H., Brezova, V., Håberg, A., 2012. The Human Brain Representation of Odor Identification.
Klingler, E., 2017. Development and organization of the evolutionarily conserved three-layered olfactory cortex. Eneuro 4.
Klockgether, T., Calderazzo-Filho, L.S., Bortolotto, Z.A., Turski, L., Cavalheiro, E.A., Turski, W.A., Ikonomidou, C., 1989. The Basal Ganglia, the Deep Prepyriform Cortex, and Seizure Spread: Bicuculline Is Anticonvulsant in the Rat Striatum.
Kowiański, P., Dziewiątkowski, J., Kowiańska, J., Moryś, J., 1999. Comparative anatomy of the claustrum in selected species: a morphometric analysis. Brain Behav. Evol. 53, 44–54.
Krettek, J.E., Price, J.L., 1977. The cortical projections of the mediodorsal nucleus and adjacent thalamic nuclei in the rat. J. Comp. Neurol. 171, 157.
Kulaga-Yoskovitz, J., Bernhardt, B.C., Hong, S.-J., Mansi, T., Liang, K.E., van der Kouwe, A.J.W., Smallwood, J., Bernasconi, A., Bernasconi, N., 2015. Multi-contrast submillimetric 3 Tesla hippocampal subfield segmentation protocol and dataset. Scientific Data 2, 150059.
Kuroda, M., López-Mascaraque, L., Price, J.L., 1992. Neuronal and synaptic composition of the mediodorsal thalamic nucleus in the rat: a light and electron microscopic Golgi study. J. Comp. Neurol. 326, 61–81.
Large, A.M., Vogler, N.W., Canto-Bustos, M., Friason, F.K., Schick, P., Oswald, A.-M.M., 2018. Differential inhibition of pyramidal cells and inhibitory interneurons along the rostrocaudal axis of anterior piriform cortex. Proc. Natl. Acad. Sci. U. S. A. 115, E8067–E8076.
Laufs, H., Richardson, M.P., Salek-Haddadi, A., Vollmar, C., Duncan, J.S., Gale, K., Lemieux, L., Löscher, W., Koepp, M.J., 2011. Converging PET and fMRI evidence for a common area involved in human focal epilepsies. Neurology 77, 904–910.
Legriel, S., Azoulay, E., Resche-Rigon, M., Lemiale, V., Mourvillier, B., Kouatchet, A., Troche, G., Wolf, M., Galliot, R., Dessertaine, G., Combaux, D., Jacobs, F., Beuret, P., Megarbane, B., Carli, P., Lambert, Y., Bruneel, F., Bedos, J.-P., 2010. Functional Outcome After Convulsive Status Epilepticus. pp. 2295–2303.
Leiva-Salinas, C., Quigg, M., Elias, W.J., Patrie, J.T., Flors, L., Fountain, N.B., Rehm, P.K., 2017. Earlier seizure onset and longer epilepsy duration correlate with the degree of temporal hypometabolism in patients with mesial temporal lobe sclerosis. Epilepsy Res. 138, 105–109.
Löscher, W., Ebert, U., 1996. The role of the piriform cortex in kindling. Prog. Neurobiol. 50, 427–481.
Luna, V.M., Schoppa, N.E., 2008. GABAergic Circuits Control Input-Spike Coupling in the Piriform Cortex. Society for Neuroscience, United States, pp. 8851.
Luskin, M.B., Price, J.L., 1983. The topographic organization of associational fibers of the olfactory system in the rat, including centrifugal fibers to the olfactory bulb. J. Comp. Neurol. 216, 264.
Mai, J.K., 2008. Atlas of the Human Brain. Elsevier, Acad. Press.
Mazo, C., Grimaud, J., Shima, Y., Murthy, V.N., Lau, C.G., 2017. Distinct Projection Patterns of Different Classes of Layer 2 Principal Neurons in the Olfactory Cortex.
Milardi, D., Cacciola, A., Calamuneri, A., Ghilardi, M.F., Caminiti, F., Cascio, F., Andronaco, V., Anastasi, G., Mormina, E., Arrigo, A., Bruschetta, D., Quartarone, A., 2017. The olfactory system revealed: non-invasive mapping by using constrained spherical deconvolution tractography in healthy humans. Frontiers in Neuroanatomy 11.
Mizobuchi, M., Ito, N., Tanaka, C., Sako, K., Sumi, Y., Sasaki, T., 1999. Unidirectional Olfactory Hallucination Associated with Ipsilateral Unruptured Intracranial Aneurysm. RAVEN PRESS PUBLISHERS, Netherlands, pp. 516.
Mufson, E.J., Mesulam, M.M., Pandya, D.N., 1981. Insular interconnections with the amygdala in the rhesus monkey. Neuroscience 6, 1231–1248.
Neville, K.R., Haberly, L.B., 2003. Beta and Gamma Oscillations in the Olfactory System of the Urethane-Anesthetized Rat. pp. 3921–3930.
Ojima, H., Mori, K., Kishi, K., 1984. The trajectory of mitral cell axons in the rabbit olfactory cortex revealed by intracellular HRP injection. J. Comp. Neurol. 230, 77–87.
Olga, M.P., 2008. Domoic acid toxicologic pathology: a review. Marine Drugs 6 (2), 180–219 ((2008), 180).
Paxinos, G., Watson, C., 1998. The Rat Brain in Stereotaxic Coordinates/George Paxinos. Academic Press, Charles Watson. San Diego, pp. c1998.
Peng, H., Long, F., Myers, G., 2011. Automatic 3D neuron tracing using all-path pruning. Bioinformatics (Oxford, England) 27, i239–i247.
Piredda, S., Gale, K., 1985. A crucial epileptogenic site in the deep prepiriform cortex. Nature 317, 623–625.
Plailly, J., Howard, J.D., Gitelman, D.R., Gottfried, J.A., 2008. Attention to odor modulates thalamocortical connectivity in the human brain. J. Neurosci. Off. J. Soc. Neurosci. 28, 5257–5267.
Porter, J., Anand, T., Johnson, B., Khan, R.M., Sobel, N., 2005. Brain Mechanisms for Extracting Spatial Information from Smell. Elsevier Science B.V, Amsterdam., United States, pp. 581.
Powell, T.P.S., Cowan, W.M., Raisman, G., 1963. Olfactory relationships of the diencephalon. Nature 199, 710.
Price, J.L., 1985. Beyond the primary olfactory cortex: olfactory-related areas in the neocortex, thalamus and hypothalamus. Chem. Senses 10, 239.
Roch, C., Leroy, C., Nehlig, A., Namer, I.J., 2002. Magnetic Resonance Imaging in the Study of the Lithium-Pilocarpine Model of Temporal Lobe Epilepsy in Adult Rats. RAVEN PRESS PUBLISHERS, Netherlands, pp. 325.
Rodriguez, A., Ehlenberger, D.B., Hof, P.R., Wearne, S.L., 2009. Three-dimensional neuron tracing by voxel scooping. J. Neurosci. Methods 184, 169–175.
Royet, J.-P., Plailly, J., Delon-Martin, C., Kareken, D., Segebarth, C., 2003. fMRI of Emotional Responses to Odors: Influence of Hedonic Valence and Judgment, Handedness, and Gender.
Rudà, R., Bello, L., Duffau, H., Soffietti, R., 2012. Seizures in low-grade gliomas: natural history, pathogenesis, and outcome after treatments. Neuro Oncol 14 (Suppl. 4), iv55–iv64.
Russchen, F.T., Amaral, D.G., Price, J.L., 1987. The afferent input to the magnocellular division of the mediodorsal thalamic nucleus in the monkey, Macaca fascicularis. J. Comp. Neurol. 256, 175–210.
Sakurada, O., Kennedy, C., Jehle, J., Brown, J.D., Carbin, G.L., Sokoloff, L., 1978. Measurement of local cerebral blood flow with iodo[14C]antipyrine. American Journal of Physiology: Heart & Circulatory Physiology 234, H59.
Sakurai, M., Suzuki, H., Tomita, N., Sunden, Y., Shimada, A., Miyata, H., Morita, T., 2018. Enhanced neurogenesis and possible synaptic reorganization in the piriform cortex of adult rat following kainic acid-induced status epilepticus. Neuropathology 38, 135–143.
Santyr, B.G., Goubran, M., Lau, J.C., Kwan, B.Y.M., Salehi, F., Lee, D.H., Mirsattari, S.M., Burneo, J.G., Steven, D.A., Parrent, A.G., Ribaupierre, S., Hammond, R.R., Peters, T.M., Khan, A.R., 2017. Investigation of hippocampal substructures in focal temporal lobe epilepsy with and without hippocampal sclerosis at 7T. J. Magn. Reson. Imaging 1359.
Savic, I., Berglund, H., 2004. Passive perception of odors and semantic circuits. Hum. Brain Mapp. 21, 271–278.
Schmidt, M.F., Storrs, J.M., Freeman, K.B., Jack, C.R., Turner, S.T., Griswold, M.E., Mosley, T.H., 2018. A comparison of manual tracing and FreeSurfer for estimating hippocampal volume over the adult lifespan. Hum. Brain Mapp. 2500.
Schofield, B.R., 2008. Retrograde axonal tracing with fluorescent markers. Current Protocols in Neuroscience 43 (1.17.11-11.17.24).
Schwabe, K., Ebert, U., Löscher, W., 2004. The central piriform cortex: anatomical connections and anticonvulsant effect of gaba elevation in the kindling model. Neuroscience 126, 727–741.
Schwarz, L.A., Miyamichi, K., Gao, X.J., Beier, K.T., Weissbourd, B., DeLoach, K.E., Ren, J., Ibanes, S., Malenka, R.C., Kremer, E.J., Luo, L., 2015. Viral-genetic tracing of the input-output organization of a central noradrenaline circuit. Nature 88.
Sharma, A.K., Reams, R.Y., Jordan, W.H., Miller, M.A., Thacker, H.L., Snyder, P.W., 2007. Mesial temporal lobe epilepsy: pathogenesis, induced rodent models and lesions. Toxicol. Pathol. 35, 984–999.
Shipley, M., Reyes, P., 1991. Anatomy of the human olfactory bulb and central olfactory pathways. In: Laing, D.G., Doty, R.L., Breipohl, W. (Eds.), The Human Sense of Smell. Springer, Berlin Heidelberg, Berlin, Heidelberg, pp. 29–60.
Skorpil, M., Rolheiser, T., Robertson, H., Sundin, A., Svenningsson, P., 2011. Technical

note: diffusion tensor fiber tractography of the olfactory tract. Magn. Reson. Imaging 29, 289–292.
Sperk, G., Lassmann, H., Baran, H., Kish, S.J., Seitelberger, F., Hornykiewicz, O., 1983. Kainic acid induced seizures: neurochemical and histopathological changes. Neuroscience 10, 1301–1315.
Stokes, C.C.A., Isaacson, J.S., 2010. Article: from dendrite to Soma: dynamic routing of inhibition by complementary interneuron microcircuits in olfactory cortex. Neuron 67, 452–465.
Sugai, T., Yamamoto, R., Yoshimura, H., Kato, N., 2012. Multimodal cross-talk of olfactory and gustatory information in the Endopiriform nucleus in rats. Chem. Senses 37, 681–688.
Suzuki, N., Bekkers, J.M., 2006. Neural Coding by Two Classes of Principal Cells in the Mouse Piriform Cortex. Society for Neuroscience, United States, pp. 11938.
Suzuki, N., Bekkers, J.M., 2010. Distinctive Classes of GABAergic Interneurons Provide Layer-Specific Phasic Inhibition in the Anterior Piriform Cortex. Oxford University Press, United States, pp. 2971.
Suzuki, N., Bekkers, J.M., 2012. Microcircuits Mediating Feedforward and Feedback Synaptic Inhibition in the Piriform Cortex. pp. 919–931.
Teitelbaum, J.S., Zatorre, R.J., Carpenter, S., Gendron, D., Evans, A.C., Gjedde, A., Cashman, N.R., 1990. Neurologic sequelae of domoic acid intoxication due to the ingestion of contaminated mussels. N. Engl. J. Med. 322, 1781–1787.
Tham, W.W.P., Stevenson, R.J., Miller, L.A., 2011. The impact of mediodorsal thalamic lesions on olfactory attention and flavor perception. Brain Cogn. 77, 71–79.
Tiedeken, J.A., Muha, N., Ramsdell, J.S., 2013. A Cupric Silver Histochemical Analysis of domoic Acid Damage to Olfactory Pathways Following Status Epilepticus in a Rat Model for Chronic Recurrent Spontaneous Seizures and Aggressive Behavior. pp. 454–469.
Tournier, J.D., Yeh, C.-H., Calamante, F., Cho, K.-H., Connelly, A., Lin, C.-P., 2008. Resolving crossing fibres using constrained spherical deconvolution: validation using diffusion-weighted imaging phantom data. NeuroImage 42, 617–625.
Van Nieuwenhuyse, B., Raedt, R., Sprengers, M., Dauwe, I., Gadeyne, S., Carrette, E., Delbeke, J., Wadman, W.J., Boon, P., Vonck, K., 2015. Research report: the systemic kainic acid rat model of temporal lobe epilepsy: Long-term EEG monitoring. Brain Res. 1627, 1–11.
Vaquero, J.J., Kinahan, P., 2015. Positron Emission Tomography: Current Challenges and Opportunities for Technological Advances in Clinical and Preclinical Imaging Systems. ANNUAL REVIEWS, United States, pp. 385.
Vaughan, D.N., Jackson, G.D., 2014. The piriform cortex and human focal epilepsy. Front. Neurol. 5, 1–18.
Veldhuizen, M., Small, D., 2011. Modality-Specific Neural Effects of Selective Attention to Taste and Odor.
Wall, C.J., Kendall, E.J., Obenaus, A., 2000. Rapid Alterations in Diffusion-weighted Images with Anatomic Correlates in a Rodent Model of Status Epilepticus. WAVERLY PRESS INC, United States, pp. 1841.
Wang, Y., Majors, A., Najm, I., Xue, M., Comair, Y., Modic, M., Ng, T.C., 1996. Postictal alteration of sodium content and apparent diffusion coefficient in epileptic rat brain induced by Kainic acid. Epilepsia 37, 1000–1006.
Watson, G., Smith, J., Alloway, K., 2016. Interhemispheric Connections Between the Infralimbic and Entorhinal Cortices: The Endopiriform Nucleus Has Limbic Connections that Parallel the Sensory and Motor Connections of the Claustrum.
Wilson, D., 1997. Binaral Interaction to the Rat Piriform Cortex.
Winston, J.S., Gottfried, J.A., Kilner, J.M., Dolan, R.J., 2005. Integrated neural representations of odor intensity and affective valence in human amygdala. J. Neurosci. 25, 8903.
Winston, G.P., Cardoso, M.J., Williams, E.J., Burdett, J.L., Bartlett, P.A., Espak, M., Behr, C., Duncan, J.S., Ourselin, S., 2013. Automated hippocampal segmentation in patients with epilepsy: available free online. Epilepsia 54, 2166–2173.
Yi-Hua, H., Wang-Tso, L., Chen, C., 2007. Multiparametric MRI evaluation of kainic acid-induced neuronal activation in rat hippocampus. Brain 3124.
Young, A., Sun, Q.Q., 2009. GABAergic Inhibitory Interneurons in the Posterior Piriform Cortex of the GAD67-GFP Mouse. Oxford University Press, United States, pp. 3011.
Young, J.C., Vaughan, D.N., Paolini, A.G., Jackson, G.D., 2018. Electrical stimulation of the piriform cortex for the treatment of epilepsy: a review of the supporting evidence. Epilepsy Behav. 88, 152–161.
Zatorre, R.J., Jones-Gotman, M., Evans, A.C., Meyer, E., 1992. Functional localization and lateralization of human olfactory cortex. Nature 360, 339–340.
Zelano, C., Montag, J., Khan, R., Sobel, N., 2009. A specialized odor memory buffer in primary olfactory cortex. PLoS One 4, e4965.